

High-Spin Iron(III) Tetramethylchiroporphyrins: Structural, Magnetic, and ^1H NMR Studies[†]

Marinella Mazzanti,[‡] Jean-Claude Marchon,^{*,‡} Jacek Wojaczyński,[§] Stanisław Wołowiec,[§] Lechosław Latos-Grażyński,^{*,§} Maoyu Shang,^{||} and W. Robert Scheidt^{*,||}

Département de Recherche Fondamentale sur la Matière Condensée, SCIB/Laboratoire de Chimie de Coordination (URA CNRS 1194), CEA-Grenoble, 38054 Grenoble, France, Department of Chemistry, University of Wrocław, 14 F. Joliot-Curie St., Wrocław 50 383, Poland, and Department of Chemistry and Biochemistry, University of Notre Dame, Notre Dame, Indiana 46556

Received September 19, 1997

The chloroiron(III) complex of $\alpha\beta\alpha\beta$ -tetramethylchiroporphyrin, $\text{FeCl}(\text{TMCP})$, was prepared, and its structure was determined by X-ray crystallography. Black crystals of $\text{FeCl}(\text{TMCP})\cdot 0.72\text{CH}_2\text{Cl}_2$ form in the tetragonal space group $P4_32_12$ with $a = b = 13.245(1)$ Å and $c = 26.355(5)$ Å at 130 K with $Z = 4$. The structure shows an unusual five-coordinate high-spin iron(III) center in a strongly ruffled and domed porphyrin, with short equatorial bond distances ($\text{Fe}-\text{N}(\text{av}) = 2.034(9)$ Å), and the iron 0.64 Å out of the porphyrin mean plane toward the chlorine atom. The solid-state magnetic moment is $5.92 \mu_{\text{B}}$ at 20 K, slightly decreasing to $5.68 \mu_{\text{B}}$ at 300 K. In solution $\text{FeCl}(\text{TMCP})$ can be easily transformed to $\text{FeBr}(\text{TMCP})$ or $\text{FeOH}(\text{TMCP})$. The ^1H NMR spectra of the three species are consistent with their C_2 symmetry and $S = 5/2$ spin state. The pyrrole proton resonances are shifted downfield to 80–100 ppm at 293 K, more than in the corresponding tetraaryl derivatives. The cyclopropyl protons on C_1 , α to the porphyrin *meso* position, appear at ca. 160–200 ppm, in keeping with the nearly perpendicular orientation of the C_1 –H bond with respect to the porphyrin mean plane. The temperature dependence of the ^1H NMR spectrum of $\text{FeCl}(\text{TMCP})$ suggests substantial zero-field splitting.

Introduction

Metal complexes of chiral porphyrins are of great current interest in the context of asymmetric catalysis and chiral recognition. Recently we reported that novel “chiroporphyrins” with stereocenters close to the porphyrin ring are readily obtained from biocartol, an intermediate in the industrial synthesis of pyrethroid insecticides.¹ First- and second-row transition metal complexes of tetramethylchiroporphyrin, H_2 -TMCP, are particularly interesting as potential asymmetric catalysts in atom-transfer reactions,¹ enantioselective receptors of chiral axial ligands,² or chiral NMR shift reagents.³ Earlier we reported on the unusual electronic configuration of low-spin Fe(III) tetramethylchiroporphyrin complexes.⁴ In the present paper we describe the preparation, crystal structure, and magnetic properties of the high-spin chloroiron(III) tetramethylchiroporphyrin, as well as the paramagnetic NMR spectra of this complex and of the related bromo and hydroxo species.

Experimental Section

Materials. Reagent grade chemicals and solvents were used as received from chemical suppliers. Tetramethylchiroporphyrin was prepared by standard methods starting with biocartol.^{1,5}

General Spectroscopic Information. UV–vis spectra were recorded on a Perkin-Elmer Lambda 9. Infrared spectra were recorded on a FT-IR Perkin-Elmer 1600 spectrometer. Routine ^1H NMR spectra were obtained at ambient temperature on a Bruker AC 200 spectrometer using deuterated chloroform solutions with CHCl_3 ($\delta = 7.24$ ppm) as an internal standard. Mass spectra were measured with a ZAB2-SEQ instrument. Elemental analyses were performed by SCA/CNRS, Vernaison, France.

FeCl(TMCP). To 50 mg (0.061 mmol) of tetramethylchiroporphyrin dissolved in 15 mL of chloroform was added 15 mL of a saturated solution of FeCl_2 in ethanol. The reaction mixture was heated to reflux for 4 h. The green-brown solution was evaporated to dryness, the residue was taken up in dichloromethane (50 mL) and the resulting solution was washed twice with water (50 mL), and then dried over sodium sulfate. After being reduced to a volume of 2 mL, the solution was chromatographed on a silica gel bed using a 1% solution of methanol in dichloromethane as the eluent, allowing separation of a small amount of unreacted tetramethylchiroporphyrin free base. Addition of hexane and slow evaporation afforded red/green crystals of $\text{FeCl}(\text{TMCP})$, **1**, in 70% yield: UV–vis (CH_2Cl_2) λ_{max} (nm) 430, 515, 585, 640, 700; FAB-MS(–) (3-nitrobenzyl alcohol) m/z 867 ($M - \text{Cl}$); IR ν_{max} (cm^{-1}) 367 ($\text{Fe}-\text{Cl}$).

Before the NMR measurements, a sample was redissolved in dichloromethane, a stream of gaseous HCl was then passed (2 h) through the solution, which was dried over anhydrous magnesium sulfate and filtered, and finally the solvent was removed under vacuum.

[†] Abbreviations used: TMCP = dianion of tetramethylchiroporphyrin; DPEP = dianion of deoxophylloerythroetioporphyrin; TPP = dianion of tetraphenylporphyrin; OEP = dianion of octaethylporphyrin; DPDME = dianion of deuteroporphyrin dimethyl ester.

[‡] CEA-Grenoble.

[§] University of Wrocław.

^{||} University of Notre Dame.

- (1) Veyrat, M.; Maury, O.; Faverjon, F.; Over, D. E.; Ramasseul, R.; Marchon, J. C.; Turowska-Tyrk, I.; Scheidt, W. R. *Angew. Chem., Int. Ed. Engl.* **1994**, *33*, 220.
- (2) Mazzanti, M.; Veyrat, M.; Ramasseul, R.; Marchon, J. C.; Turowska-Tyrk, I.; Shang, M.; Scheidt, W. R. *Inorg. Chem.* **1996**, *35*, 3733.
- (3) Toronto, D.; Sarrazin, F.; Pécaut, J.; Marchon, J. C.; Shang, M.; Scheidt, W. R. *Inorg. Chem.* **1998**, *37*, 526.
- (4) Wołowiec, S.; Latos-Grażyński, L.; Mazzanti, M.; Marchon, J. C. *Inorg. Chem.* **1997**, *36*, 5761.

- (5) Veyrat, M.; Fantin, L.; Desmoulins, S.; Petitjean, A.; Mazzanti, M.; Ramasseul, R.; Marchon, J. C.; Bau, R. *Bull. Soc. Chim. Fr.* **1997**, *134*, 703.

Table 1. Crystallographic Data

molecule	Fe(TMCP)Cl·0.72CH ₂ Cl ₂
chem formula	C _{48.72} H _{53.43} Cl _{2.43} FeN ₄ O ₈
fw	965.17
space group	<i>P</i> ₄ ₃ ₂ 1 (No. 96)
<i>a</i> , <i>b</i>	13.245(1) Å
<i>c</i>	26.355(5) Å
<i>V</i>	4623.4(10) Å ³
<i>Z</i>	4
<i>T</i>	−143(2) °C
<i>λ</i>	0.710 73 Å
ρ_{calcd}	1.387 g·cm ^{−3}
μ	5.25 cm ^{−1}
final <i>R</i> indices [<i>I</i> > 2 σ (<i>I</i>)] ^a	<i>R</i> ₁ = 0.0734, <i>wR</i> ₂ = 0.1574
<i>R</i> indices (all data) ^a	<i>R</i> ₁ = 0.0955, <i>wR</i> ₂ = 0.1713

^a $R_1 = \sum ||F_o| - |F_c|| / \sum |F_o|$ and $wR_2 = \{\sum [w(F_o^2 - F_c^2)^2] / \sum [wF_o^4]\}^{1/2}$. The conventional *R*-factors *R*₁ are based on *F*, with *F* set to zero for negative *F*². The criterion of $F^2 < 2\sigma(F^2)$ was used only for calculating *R*₁. *R*-factors based on *F*² (*wR*₂) are statistically about twice as large as those based on *F*, and *R*-factors based on all data will be even larger.

Fe(OH)(TMCP). A solution of FeCl(TMCP) in benzene was passed through wet basic alumina. Elution with acetone/benzene (5/95 v/v) and removal of the solvent on the rotary evaporator yielded Fe(OH)(TMCP) as a violet powder. In an alternative procedure, a benzene solution of FeCl(TMCP) was stirred with aqueous NaOH, the organic layer was separated, dried over anhydrous sodium sulfate, and filtered, and the filtrate was evaporated to dryness.

FeBr(TMCP). A benzene solution of Fe(OH)(TMCP) was stirred with 1 M aqueous HBr. The organic layer was separated, dried over anhydrous magnesium sulfate and filtered, and the solvent was removed under vacuum.

X-ray Structure Determination. Data collection for a black crystal of [FeCl(TMCP)](CH₂Cl₂)_{0.72} (**1**) was carried out on an Enraf-Nonius FAST area detector diffractometer at 130 K with our standard methods for small molecules.⁶ A brief summary of determined parameters is given in Table 1 and Table S1. A total of 35 128 reflections were collected, of which 6233 were unique, and intensities of 5028 unique reflections were larger than 2.0 σ (*I*). All reflections were corrected for Lorentz–polarization factors. The structure was solved by the direct methods SHELXS-86 program.⁷ All non-hydrogen atoms were shown on an E-map except the dichloromethane solvent, which was found in succeeding difference Fourier synthesis. The solvent is disordered with the carbon atom located nicely on a 2-fold axis with two independent chlorine atoms that were disordered on two sets of positions around the 2-fold axis. After the non-hydrogen atoms were refined to convergence anisotropically,⁷ a difference Fourier map showed most of the hydrogen atoms. These hydrogen atoms were included in the final refinement as idealized atoms with standard SHELXL idealizations. The structure was refined against *F*² by the SHELXL-93 program.⁷ The refinement converged to a final value of *R*₁ = 0.0734 and *wR*₂ = 0.1574 for observed unique reflections (*I* ≥ 2.0 σ (*I*)) and *R*₁ = 0.0955 and *wR*₂ = 0.1713 for all unique reflections including those with negative intensities. The weighted *R*-factors, *wR*₂, are based on *F*², and conventional *R*-factors, *R*, on *F*, with *F* set to zero for negative intensities. All reflections, including those with negative intensities, were included in the refinement, and the *I* ≥ 2.0 σ (*I*) criterion was used only for calculating *R*₁. The maximum and minimum residual electron densities on the final difference Fourier map were 0.669 and −0.954 e/Å³, respectively. The correctness of the chosen enantiomorph was confirmed by a near zero Flack absolute structure parameter of

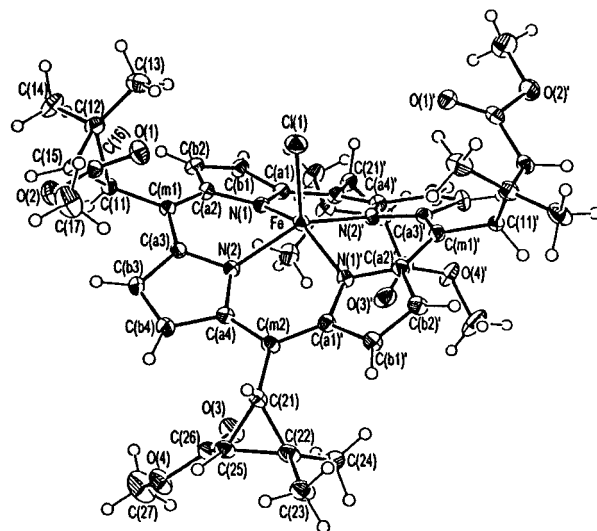


Figure 1. ORTEP diagram of FeCl(TMCP) with the atom-labeling scheme. Thermal ellipsoids are drawn at the 50% probability level for the structure determined at 130 K.

−0.02(3).⁸ Final atomic coordinates are listed in Table S2 (Supporting Information).

Magnetic Susceptibility Measurements. The solid-state magnetic susceptibilities were measured under helium on a Quantum Design MPMS SQUID susceptometer from 2 to 300 K at a field of 0.5 T. The sample was contained in a Kel-F bucket. The bucket had been calibrated independently at the same field and temperatures. The raw data were corrected for the diamagnetic contribution of both the sample holder and the compound to the susceptibility, using Pascal's constants for the metal and axial ligand atoms, and a calculated value $\chi_M = -638 \times 10^{-6}$ cgs emu for H₂(TMCP).

NMR and EPR Spectroscopies. ¹H NMR spectra were recorded on a Bruker AMX spectrometer operating in the quadrature mode at 300 MHz. The residual ¹H NMR resonances of deuterated solvents were used as a secondary reference. An inversion–recovery sequence was used to suppress the diamagnetic signals in selected spectra. EPR spectra were obtained with a Bruker ESP 300E spectrometer. The magnetic field was calibrated with a proton magnetometer and EPR standards.

Results and Discussion

X-ray Structure. A view of the complex is shown in Figure 1. Atomic positional parameters are given in Table 2. Complete listings of bond distances and angles are included in the Supporting Information.

The porphyrin ring in **1** is strongly ruffled in order to accommodate the alternating up, down *meso* cyclopropyl substituents. However, an additional core deformation is also apparently required to accommodate the high-spin iron(III) atom (vide infra). A formal diagram of the porphyrinato core showing the pattern of displacements of atoms from the least-squares 24-atom plane (in units of 0.01 Å) is given in Figure 2. Also shown in this figure are averaged values of bond distances and angles in the core. The out-of-plane displacements from the 24-atom macrocyclic core for the two unique *meso* carbon atoms are C₅ = −0.69 Å and C₁₀ = 0.67 Å. The angles between adjacent pyrrole rings of the porphyrin are 23.7, 42.1, and 34.7°. The methyl ester groups lie on the porphyrin ring with the carbonyl oxygen atoms nearly eclipsing the four α -pyrrole carbons. The carbonyl and one methyl of the *gem*-dimethyl group in two opposite cyclopropyl groups define a C₂-symmetric

(6) Scheidt, W. R.; Turowska-Tyrk, I. *Inorg. Chem.* **1994**, *33*, 1314.

(7) Programs used in this study included the following: SHELXS-86 (Sheldrick, G. M. *Acta Crystallogr., Sect. A* **1990**, *46*, 467); SHELXL-93 (Sheldrick, G. M. *J. Appl. Crystallogr.*, manuscript in preparation); local modifications of Johnson's ORTEP2. Scattering factors were taken from the following: *International Tables for Crystallography*; Wilson, A. J. C., Ed.; Kluwer Academic Publishers: Dordrecht, The Netherlands, 1992; Vol. C.

(8) Flack, H. D. *Acta Crystallogr., Sect. A* **1983**, *39*, 876.

Table 2. Atomic Coordinates and Equivalent Isotropic Displacement Parameters U_{eq} (\AA^2) for $\text{Fe}(\text{TMCP})\text{Cl}\cdot 0.72\text{CH}_2\text{Cl}_2$

	<i>x</i>	<i>y</i>	<i>z</i>	U_{eq} (\AA^2) ^a
Fe	0.48544(4)	0.48544(4)	0.0000	0.0203(2)
Cl(1)	0.60326(7)	0.60326(7)	0.0000	0.0320(3)
N(1)	0.3561(3)	0.5567(2)	0.02029(11)	0.0206(6)
N(2)	0.4822(2)	0.4266(2)	0.07151(10)	0.0205(6)
C(a1)	0.2779(3)	0.5908(3)	-0.00880(14)	0.0226(8)
C(a2)	0.3476(3)	0.6035(3)	0.06672(13)	0.0214(7)
C(a3)	0.4548(3)	0.4842(3)	0.11261(12)	0.0210(7)
C(a4)	0.5209(3)	0.3386(3)	0.08984(13)	0.0229(7)
C(b1)	0.2195(3)	0.6617(3)	0.01989(15)	0.0254(8)
C(b2)	0.2647(3)	0.6717(3)	0.06572(15)	0.0257(8)
C(b3)	0.4787(3)	0.4296(3)	0.15829(13)	0.0261(8)
C(b4)	0.5164(4)	0.3391(3)	0.14395(14)	0.0293(8)
C(m1)	0.4018(3)	0.5746(3)	0.10984(12)	0.0212(7)
C(m2)	0.5665(3)	0.2637(3)	0.06014(14)	0.0230(8)
C(11)	0.3885(3)	0.6368(3)	0.15681(12)	0.0211(7)
C(12)	0.4209(3)	0.7450(3)	0.1602(2)	0.0271(8)
C(13)	0.4724(4)	0.7959(4)	0.1163(2)	0.0370(10)
C(14)	0.3506(4)	0.8142(4)	0.1901(2)	0.0379(11)
C(15)	0.4768(3)	0.6659(3)	0.19157(14)	0.0243(8)
C(16)	0.5808(3)	0.6315(3)	0.18005(14)	0.0251(8)
O(1)	0.6235(2)	0.6357(3)	0.13997(10)	0.0331(7)
O(2)	0.6227(2)	0.5939(3)	0.22247(10)	0.0347(7)
C(17)	0.7226(4)	0.5514(5)	0.2156(2)	0.0484(14)
C(21)	0.6056(3)	0.1699(3)	0.08554(14)	0.0249(8)
C(22)	0.5824(3)	0.0655(3)	0.0679(2)	0.0286(9)
C(23)	0.6680(4)	-0.0102(4)	0.0714(2)	0.0376(11)
C(24)	0.5109(4)	0.0452(3)	0.0240(2)	0.0358(10)
C(25)	0.5400(3)	0.1009(3)	0.11867(15)	0.0264(8)
C(26)	0.4311(3)	0.1166(3)	0.1254(2)	0.0299(9)
O(3)	0.3721(2)	0.1519(3)	0.09608(12)	0.0400(8)
O(4)	0.4037(3)	0.0839(3)	0.17202(12)	0.0415(9)
C(27)	0.2973(4)	0.0935(6)	0.1834(2)	0.060(2)
C(1)	0.2913(5)	0.2913(5)	0.0000	0.041(2) ^b
Cl(2)	0.2529(7)	0.1948(6)	-0.0331(4)	0.121(3) ^b
Cl(3)	0.2207(6)	0.3296(8)	0.0453(3)	0.123(3) ^b

^a $U_{eq} = (1/3)\sum_i U_{ij} a_i^* a_j^* a_i \cdot a_j$. ^b Occupancy coefficient was 0.358(4).

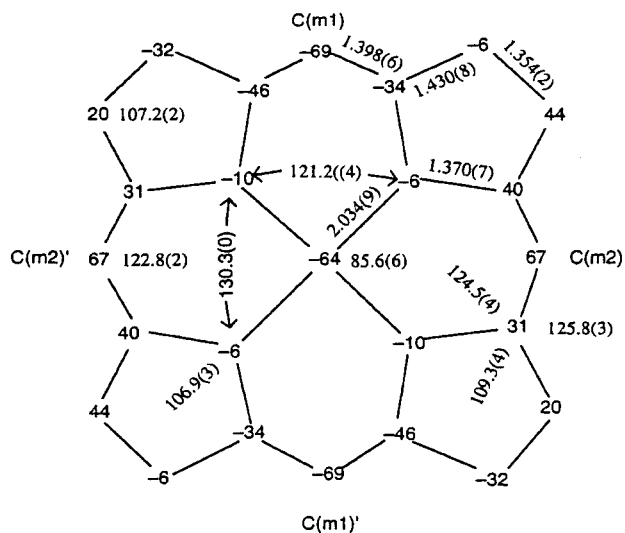


Figure 2. Formal diagram of the porphinato core showing the pattern of displacements of atoms from the least-squares 24-atom plane in units of 0.01 Å. Averaged values of bond distances and angles in the core are also shown.

groove which accommodates the axial ligand on one face of the porphyrin.

The iron atom is displaced from the porphyrin mean plane toward the chlorine atom; the Fe–Cl distance (0.64 Å) is as large as that in any other high-spin iron(III) porphyrin.^{9a,b} Despite this very large iron atom displacement, the average Fe–N distance is 2.034 Å, much shorter than the nominal 2.065

Å value. It is indeed shorter than any of those previously observed for five-coordinate high-spin iron(III) porphyrin derivatives.^{9c} In fact, the distance is shorter than those observed in six-coordinate high-spin iron(III) porphyrins, where Fe–N ≥ 2.045 Å even though the iron(III) is centered or nearly centered in the porphyrin plane.^{9d–h} However, this average Fe–N distance is much larger than that observed in intermediate-spin iron(III) porphyrins in which the $d_{x^2-y^2}$ orbital is unoccupied,⁹ⁱ where Fe–N ≈ 1.929 Å, and thus a quartet ($S = 3/2$) ground state can be ruled out. It is possible that **1** has some small $S = 3/2$ character in its electronic structure, which could be correlated to a smaller Fe–N distance, akin to that recently reported for two highly distorted five-coordinate iron(III) complexes with admixed ground states.^{9j} However, the ground state for **1** must largely be that of an $S = 5/2$ state as shown by the magnetic susceptibility and ¹H NMR data (vide infra).

The core conformation in the strongly pyramidal FeN_4Cl coordination group of **1** is most unusual for a high-spin iron(III) derivative. As was noted above, the core displays a substantial ruffling to accommodate the four bulky *meso* substituents. A well-known consequence of such ruffling is significantly shortened equatorial bonds.^{9k} A second set of deformations is needed to satisfy the coordination requirements of high-spin iron(III). These are the large out-of-plane displacement of iron and a doming of the core. As can be seen from an examination of the atomic displacements shown in Figure 2, a C_{4v} doming of the core is superimposed on the more predominant S_4 ruffling. C_{4v} domed cores are relatively unusual, but the combination of substantial doming and ruffling has been observed only rarely.^{9l} The combination apparently represents the best solution to the steric problem of accommodating the large iron(III) atom. Some of the needed distortion in the core can be seen in the disparate values observed for the Fe–N–C_a bond angles (Figure 2) that are seen to differ by almost 10° at each nitrogen atom. Finally we note that a different solution has been seen for five-coordinate zinc in another chirophyrin derivative which contains pendant *p*-nitrophenyl groups (“Venus flytrap porphyrin”).¹⁰ In this molecule, the porphyrin atropisomerizes to the $\alpha\alpha\alpha\alpha$ conformer from the $\alpha\beta\alpha\beta$ in response to binding a pyridine axial ligand. That **1** does not also atropisomerize to alleviate its steric difficulties points to the significance of the secondary interactions involving the porphyrin pendant groups and the axial ligand in the Venus flytrap porphyrin.

Magnetism. The magnetic moment μ_{eff} measured in the 20–300 K interval (Figure S7, Supporting Information) is close to the spin-only value expected for a high-spin $S = 5/2$ system: μ_{eff} is equal to 5.92 μ_B at 20 K, and it slightly decreases to 5.68 μ_B at 300 K. Below 20 K, the magnetic moment drops rapidly,

- (9) (a) Phillippi, M. A.; Baenziger, N.; Goff, H. M. *Inorg. Chem.* **1981**, *20*, 3904. (b) Gold, A.; Jayaraj, K.; Doppelt, P.; Fischer, J.; Weiss, R. *Inorg. Chim. Acta* **1988**, *150*, 177. (c) Scheidt, W. R.; Gouterman, M. In *Iron Porphyrins Part I*, Lever, A. B. P., Gray, H., Eds.; Addison-Wesley: Reading, MA, 1983; p 89. (d) Mashiko, T.; Kastner, M. E.; Spartalian, K.; Scheidt, W. R.; Reed, C. A. *J. Am. Chem. Soc.* **1978**, *100*, 6354. (e) Scheidt, W. R.; Cohen, I. A.; Kastner, M. E. *Biochemistry* **1979**, *18*, 3546. (f) Buisson, G.; Deronzier, A.; Duée, E.; Gans, P.; Marchon, J.-C.; Regnard, J.-R. *J. Am. Chem. Soc.* **1982**, *104*, 6793. (g) Geiger, D. K.; Lee, Y. J.; Scheidt, W. R. *J. Am. Chem. Soc.* **1984**, *106*, 6339. (h) Scheidt, W. R.; Geiger, D. K.; Lee, Y. J.; Gans, P.; Marchon, J.-C. *Inorg. Chem.* **1992**, *31*, 2660. (i) Fitzgerald, J. P.; Haggerty, B. S.; Rheingold, A. L.; May, L.; Brewer, G. A. *Inorg. Chem.* **1992**, *31*, 2006. (j) Cheng, R.-J.; Chen, P.-Y.; Gau, P.-R.; Chen, C.-C.; Peng, S.-M. *J. Am. Chem. Soc.* **1997**, *119*, 2563. (k) Hoard, J. L. *Ann. N.Y. Acad. Sci.* **1973**, *206*, 18. (l) Senge, M. O.; Ema, T.; Smith, K. M. *J. Chem. Soc., Chem. Commun.* **1995**, 733.
- (10) Mazzanti, M.; Marchon, J. C.; Shang, M.; Scheidt, W. R.; Jia, S.; Shelnutz, J. A. *J. Am. Chem. Soc.* **1997**, *119*, 12400.

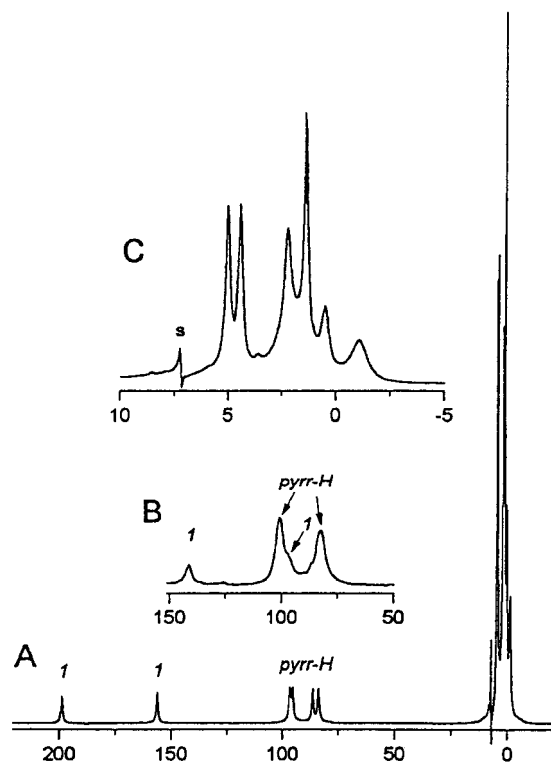
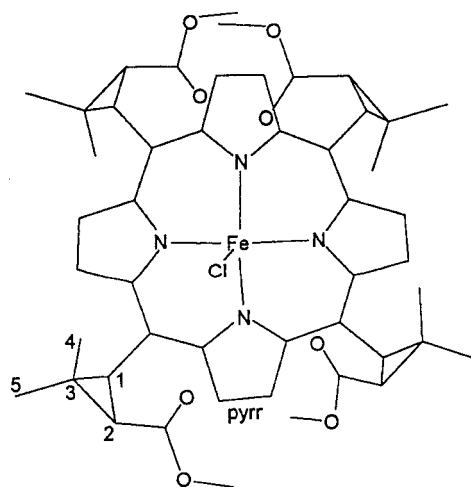


Figure 3. ^1H NMR spectra of (A) $\text{FeCl}(\text{TMCP})$; (B) $\text{Fe}(\text{OH})(\text{TMCP})$, downfield region, and (C) methyl resonances of $\text{FeCl}(\text{TMCP})$ in the 7 to -3 ppm region. All spectra have been taken in chloroform- d at 293 K. Labeling: *pyrr-H*, pyrrole protons; *1*, 1-CH of the *meso* alkyl substituent. The spectra were obtained under T_1 inversion–recovery conditions with rapidly relaxing paramagnetic resonances appearing in the normal phasing.

reflecting the large zero-field splitting of the ground state which is usual in high-spin iron(III) porphyrins.¹¹ The EPR spectrum of $\text{FeCl}(\text{TMCP})$ in a frozen CDCl_3 solution at 3.5 K shows the usual features of the $S = 5/2$ electronic state with strong $g_{\perp} = 6$ and weak $g_{\parallel} = 2$ signals.¹²

^1H NMR Studies. Our analysis of the complex spectra of $\text{FeCl}(\text{TMCP})$ and its two other high-spin analogues relates directly to the geometric information available from the X-ray studies. The molecule appears to have effective C_2 symmetry in solution with the C_2 axis passing through the iron atom and the axial chloride (see above). Accordingly there are four distinct pyrrole positions and two *meso* positions, and each type of alkyl *meso* substituent is expected to contribute three methine and two methylene resonances. The ^1H NMR spectrum of $\text{FeCl}(\text{TMCP})$ is shown in Figure 3. The resonance assignments which are given above selected peaks have been made on the basis of relative intensities and line width analysis. The labeling is made according to Chart 1.

Chart 1



The resonances observed at 293 K may be separated into three groups. The four well-defined pyrrole resonances are shifted downfield to the 80–100 ppm, markedly more downfield than for the five-coordinate high-spin iron(III) tetrarylporphyrins which exhibit the pyrrole resonance at 80 ppm.¹³ This increased shift might result from geometric (ruffled and domed core vs domed only) or electronic (alkyl vs aryl *meso* substituents) differences or from a combination of geometric and electronic effects. In any event, the highly downfield-shifted pyrrole resonances of **1** are inconsistent with an intermediate or admixed spin state.¹⁴ Two other resonances at 156.3 and 198.9 ppm are assigned as the methine 1-CH protons of the *meso* substituents. By default the remaining paramagnetically shifted resonances, located in the crowded 6 to -3 ppm region, are assigned to the other protons of the *meso* alkyl groups (Figure 3, trace C). The large downfield shifts of 1-CH protons, although apparently unusual, merely reflect their specific orientation with respect to the porphyrin macrocycle. This orientation is conveniently described by the dihedral angle ϕ between the plane determined by the p_z axis of the *meso* carbon (C_{meso}) and the $C_{\text{meso}}-C_1$ bond and that determined by C_{meso} and the C_1-H bond. The values of ϕ obtained from the X-ray structure of **1** are 0.9 and 7.2° , reflecting the desire of the bulky substituents of the *meso* cyclopropyl fragment to be located as far away as possible from the porphyrin plane. Theoretically the contact shift of methine proton equals $Q \cos^2 \phi \rho / K$, where Q and K are constants and ρ is spin density at a *meso* position.¹⁵ The contact shift approaches its maximal value for the conformation of $\text{FeCl}(\text{TMCP})$ which is observed in the solid state. A similar geometry was found in the iron(III) complexes of isocyclic porphyrins. Thus, for the rigid five-membered isocyclic ring of $\text{FeI}(\text{DPEP})$ with $\phi = 30^\circ$ the methylene resonances at the *meso* position are located at 118.2 and 130.8 ppm.¹⁶ Similarly, the 15- CH_2 resonances were observed in the 160–180 ppm region for an iron(III) derivative of chlorophyll *a* (pyrphosphorobide *a* methyl ester).¹⁷

The 2-CH resonances of $\text{FeCl}(\text{TMCP})$ probably overlap with the methyl peaks and have not been identified. The dominant

- (11) Large ligand field splitting has been reported in a number of high-spin iron(III) porphyrins and heme proteins. In zero field, the 6A_1 state is split into three doublets with $S_z = \pm 1/2, \pm 3/2$, and $\pm 5/2$ with energies 0, $2D$, and $6D$, respectively. At very low temperatures most of the spins are in the $|\pm 1/2\rangle$ state. See for example: (a) Johnson, C. E. *Phys Lett.* **1966**, *21*, 491. (b) Tang, S. C.; Koch, S.; Papaefthymiou, G. C.; Foner, S.; Frankel, R. B.; Ibers, J. A.; Holm, R. H. *J. Am. Chem. Soc.* **1976**, *98*, 2414. (c) Ernst, J.; Subramanian, J.; Fuhrhop, J. H. *Z. Naturforsch.* **1977**, *32a*, 1129. (d) Mitra, S. In *Iron Porphyrins Part II*; Lever, A. B. P., Gray, H., Eds., Addison-Wesley: Reading, MA, 1983; p 1. For a theoretical description of the magnetic susceptibility of these zero-field split systems, see: (e) Weissbluth, M. *Struct. Bonding (Berlin)* **1966**, *2*, 1.
- (12) Palmer, G. In *Iron Porphyrins Part II*; Lever, A. B. P., Gray, H., Eds.; Addison-Wesley: Reading, MA, 1983; p 43.

- (13) Walker, F. A.; Simonis, U. In *Biological Magnetic Resonance, Volume 12: NMR of Paramagnetic Molecules*; Berliner, L. J., Reuben, J., Eds.; Plenum Press: New York, 1993; p 133.
- (14) Reed, C. A.; Guiset, F. *J. Am. Chem. Soc.* **1996**, *118*, 8, 3281.
- (15) Pignolet, L. H.; La Mar, G. N. In *NMR of Paramagnetic Molecules*; La Mar, G., Horrocks, W. D., Jr., Holm, R. H., Eds.; Academic Press: New York, 1973; p 357.
- (16) Wolowicz, S.; Latos-Grażyński, L.; Serebrennikova, O. V.; Czechowski, F. *Magn. Reson. Chem.* **1995**, *33*, 34.
- (17) Licoccia, S.; Chatfield, M. J.; La Mar, G. N.; Smith, K. M.; Mansfield, K. E.; Anderson, R. R. *J. Am. Chem. Soc.* **1989**, *111*, 6087.

Table 3. ^1H NMR Data^a

compd	δ (ppm)		
	pyrrole-H	1-CH	CH ₃
FeCl(TMCP)	96.7 (320), 95.6 (320), 86.5 (250), 83.9 (240)	198.9 (300), 156.3 (260)	5.1 (50), 4.5 (50), 2.3 (110), 1.4 (40), 0.6 (120), -1.0 (240)
FeBr(TMCP)	89.5 (170), 88.5 (160), 81.4 (150), 78.9 (150)	197.0 (150), 160.1 (140)	6.0 (40), 5.3 (50), 3.7 (30), 2.5-0.8, -1.6 (180)
FeOH(TMCP)	101.0, 82.8	141.4, 97.0	5 to (-2)

^a All spectra measured in chloroform-*d* at 293 K. Line widths (Hz) given in parentheses.

relaxation mechanism for the methyl protons is due to dipolar interaction, which leads to relative line widths proportional to r^{-6} , where r is the iron-proton distance averaged over all acquired positions.¹⁸ Values of r have been extracted from the crystallographic data. The relevant line widths have been obtained by a deconvolution procedure, and they exhibit a rather large spread (Table 3). However, the flexibility of the *meso* substituents renders an unambiguous assignment based solely on the line width analysis very difficult.

The observed shifts of the pyrrole and 1-CH protons of FeCl(TMCP) are consistent with the scheme previously proposed for high-spin iron porphyrins, wherein a σ -delocalization (porphyrin $3e(\pi) \rightarrow \text{metal } d$) distributes positive spin density to the β -pyrrole positions and a metal-to-porphyrin π -donation (back-bonding) into the $4e(\pi^*)$ orbitals is reflected by *meso* substituent shifts.¹⁹ The strong downfield contribution of the σ -mechanism usually is dominant for high-spin iron(III) porphyrins.²⁰

The isotropic shifts of the *meso* methyl resonances do not fall in one direction. A dipolar shift due to the ZFS term typically observed for high-spin iron(III) porphyrins^{13,19} can account for this observed upfield and downfield spread of methyl resonances. Thus, the relative shifts can parallel the computed values of the geometric factors $(3 \cos^2 \theta - 1)/r^3$, and opposite signs of the dipolar shifts could be expected for methyl resonances with θ values smaller or larger than the magic angle (54°). However, a more quantitative analysis seems to be pointless as the flexibility of the *meso* alkyl fragment requires a population-averaged geometric factor, and it would be complicated by the fact that upfield shifted resonances correspond to protons with θ values close to the magic angle. One has also to keep in mind that a substantial contact contribution can be expected for *meso* alkyl substituents.

The temperature dependence of the ^1H NMR spectrum of FeCl(TMCP) is shown in Figure 4. The departure from the Curie law is a result of the zero-field splitting and can be accounted for by using eq 1, where $\Delta H/H_{\text{iso}}$ is the isotropic shift,

$$\Delta H/H_{\text{iso}} = \alpha/T + \beta/T^2 \quad (1)$$

$\alpha = -A/h[35g\mu_B/(12k\gamma_H/2\pi)]$, and $\beta = 28g^2\mu_B(3 \cos^2 \theta - 1)D/9k^2r^3$. Using the computed geometric factors, the data can be fit to this equation to yield $A/h = 1.88 \cdot 10^5$ Hz for pyrrole resonances and $D = 29 \text{ cm}^{-1}$. The D value is much larger than those ($6\text{--}9 \text{ cm}^{-1}$) typically found for the corresponding TPP, OEP, and DPDME complexes,¹¹ and it may reflect the fact that the dipolar contributions are much larger than usual. However,

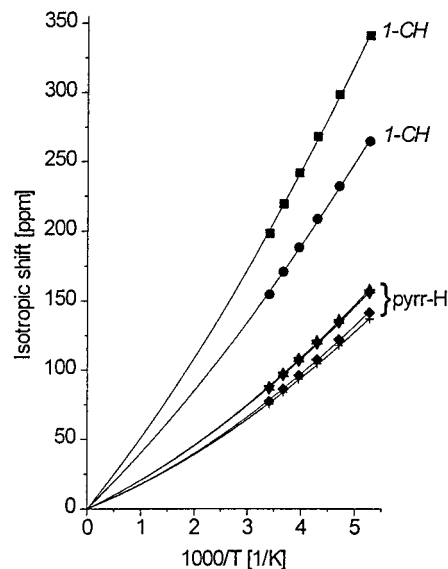


Figure 4. Plots of the isotropic shifts of pyrrole and 1-CH resonances for FeCl(TMCP) as a function of $1/T$. The isotropic shifts have been determined using $\text{Ru}(\text{CO})(\text{EtOH})(\text{TMCP})$ as a diamagnetic reference.² Labeling follows those from Figure 3. The solid lines are included for illustrative purposes only.

further studies of tetraalkyl derivatives are required before this interpretation can be accepted.

In addition to FeCl(TMCP) and FeBr(TMCP) (see Table 3), we have also investigated the hydroxo complex FeOH(TMCP). The existence of this complex is readily established by ^1H NMR (Figure 3, trace B), and its stability is attributed to steric effects which prevent the formation of the corresponding (μ -oxo)diiron(III) complex.²¹ The ^1H NMR spectrum of FeOH(TMCP) resembles that of FeCl(TMCP) as far as the positions of pyrrole resonances are concerned. The resonances of 1-CH group are downfield shifted, although the extent of the shift is considerably smaller when compared to the chloro species. All lines are broader than those found for the corresponding chloride and bromide complexes, which is typically observed in any series of high-spin iron(III) porphyrins.^{13,21,22} The markedly smaller shifts of 1-CH resonances may be explained by two factors: lower contact shifts at the *meso* carbon or higher values of the dihedral angle ϕ describing the position of the *meso* substituent (see above). The formation of a hydrogen bond between the hydroxo ligand and a carbonyl oxygen on the side of the groove may be instrumental in this mechanism. We have used molecular mechanics (HYPERCHEM) to construct a model which demonstrates that the hydrogen-bonding distance is easily attained by a small rotation with respect to the *meso* (1-C) bond. This type of interaction with a hydrogen bond donor on an axial

(18) Swift, T. J. In *NMR of Paramagnetic Molecules*; La Mar, G., Horrocks, W. D., Jr., Holm, R. H., Eds.; Academic Press: New York, 1973; pp 53-83.

(19) La Mar, G. N.; Eaton, G. R.; Holm, R. H.; Walker, F. A. *J. Am. Chem. Soc.* **1973**, *95*, 63.

(20) Wojaczyński, J.; Latos-Grażyński, L.; Hrycyk, W.; Pacholska, E.; Rachlewicz, K.; Szyrenberg, L. *Inorg. Chem.* **1996**, *35*, 6861.

(21) Cheng, R.-J.; Latos-Grażyński, L.; Balch, A. L. *Inorg. Chem.* **1982**, *21*, 2412.

(22) La Mar, G. N.; Walker, F. A. *J. Am. Chem. Soc.* **1973**, *95*, 6950.

ligand is structurally well documented in the TMCP series for a ruthenium(II)–ethanol complex² and a cobalt(III)–amine complex.³

Summary

Results from this investigation suggest that the effects of a small porphyrin “hole” size on the spin state of five-coordinate iron(III) complexes can be very subtle. As a result of a strongly ruffled porphyrin conformation, FeCl(TMCP) (**1**) has an average Fe–N_{av} bond distance (2.034 Å) which is much shorter than the nominal 2.065 Å value, and yet its high-spin ground state is clearly reflected in the value of its magnetic moment and in the large downfield shifts of its ¹H NMR resonances. Thus, **1** appears as a structurally unusual member in the class of five-coordinate high-spin iron(III) porphyrin complexes. In contrast, the five-coordinate chloroiron(III) complexes of two highly distorted octaalkyltetraphenylporphyrins with Fe–N_{av} = 2.031 and 2.034 Å exhibit admixed ⁵/₂, ³/₂ ground states.^{9j} An extreme case is that of the chloroiron(III) complex of octaethyltetraaza-porphyrin in which the very small porphyrin “hole” size results

in an unoccupied d_{x²-y²} orbital (Fe–N_{av} = 1.929 Å) and in a stabilization of the pure intermediate ³/₂ state.⁹ⁱ

Acknowledgment. Work at Grenoble was supported by the CEA, the CNRS (Grant URA 1194), and the European Union, at Wrocław by the KBN (Grant 3 T09A 14309), and at Notre Dame by the NIH (Grants GM-38401 and RR-06709). M.M. thanks the Human Capital and Mobility program of the EU for a postdoctoral fellowship. We are indebted to Patrick Dubourdeaux for assistance with the syntheses of the compounds. J.-C.M. wishes to thank Professor James P. Collman for his generous hospitality at Stanford University, where this paper was written, and Steven Harford for critical reading of the manuscript.

Supporting Information Available: Tables S1–S6, listing complete crystallographic details, atomic coordinates, bond lengths, bond angles, anisotropic thermal parameters, and fixed hydrogen atom positions, and Figure S7, showing a plot of μ_{eff} vs T for **1** (11 pages). Ordering information is given on any current masthead page.

IC9711933